

Hidden Markov models as recurrent neural networks: An application to Alzheimer’s disease

1st Matt Baucum

Industrial & Systems Engineering
University of Tennessee
Knoxville, TN, U.S.A.
mbaucum1@vols.utk.edu

2nd Anahita Khojandi

Industrial & Systems Engineering
University of Tennessee
Knoxville, TN, U.S.A.
khojandi@utk.edu

3rd Theodore Papamarkou

Department of Mathematics
The University of Manchester
Manchester, U.K.
Computational Sciences & Engineering Division
Oak Ridge National Laboratory
Oak Ridge, TN, U.S.A.
theodoros.papamarkou@manchester.ac.uk

Abstract—Hidden Markov models (HMMs) are commonly used for disease progression modeling when the true patient health state is not fully known. Since HMMs may have multiple local optima, performance can be improved by incorporating additional patient covariates to inform estimation. To allow for this, we develop hidden Markov recurrent neural networks (HMRNNs), a special case of recurrent neural networks with the same likelihood function as a corresponding discrete-observation HMM. The HMRNN can be combined with any other predictive neural networks that take patient information as input, with all parameters estimated simultaneously via gradient descent. Using a dataset of Alzheimer’s disease patients, we demonstrate how combining the HMRNN with other predictive neural networks improves disease forecasting performance and offers a novel clinical interpretation compared with a standard HMM trained via expectation-maximization.

Index Terms—hidden Markov models, neural networks, disease progression

I. INTRODUCTION

Hidden Markov models (HMMs; [1]) are commonly used for modeling disease progression, because they capture complex and noisy clinical measurements as originating from a smaller set of latent health states. Because of their intuitive parameter interpretations and flexibility, HMMs have been used to model sepsis [2], Alzheimer’s disease progression [3], and patient response to blood anticoagulants [4].

Researchers may wish to use patient-level covariates to improve the fit of HMM parameter solutions [5], or to integrate HMMs directly with treatment planning algorithms [4]. Either modification requires incorporating additional parameters into the HMM, which is typically intractable with expectation-maximization algorithms. Incorporating covariates or additional treatment planning models therefore requires multiple estimation steps (e.g., [5]) changes to HMM parameter interpretation (e.g., [4]), or Bayesian estimation, which involves joint prior distributions over all parameters and can suffer from poor convergence in complex models [6].

We present neural networks as a valuable alternative for implementing and solving HMMs for disease progression modeling. Neural networks’ substantial modularity allows them to easily incorporate additional input variables (e.g., patient-level covariates) or predictive models and simultaneously

estimate all parameters [7]. We therefore introduce Hidden Markov Recurrent Neural Networks (HMRNNs) - neural networks that mimic the computation of hidden Markov models while allowing for substantial modularity with other predictive networks. In doing so, our primary contributions are as follows: (1) We prove how recurrent neural networks (RNNs) can be formulated to optimize the same likelihood function as HMMs, with parameters that can be interpreted as HMM parameters (section III), and (2) we demonstrate the HMRNN’s utility for disease progression modeling, in which combining it with other predictive neural networks improves predictive accuracy and offers unique parameter interpretations not afforded by simple HMMs (section IV).

II. RELATED WORK

A few studies in the speech recognition literature model HMMs with neural networks [8], [9]; these implementations require HMM pre-training [8] or minimize the mutual information criterion [9], and they are not commonly used outside the speech recognition domain. These works also present only theoretical justification, with no empirical comparisons with expectation-maximization algorithms.

A limited number of healthcare studies have also explored connections between neural networks and Markov models. [4] employs a recurrent neural network to approximate latent health states underlying patients’ ICU measurements. [10] compares HMM and neural network effectiveness in training a robotic surgery assistant, while [11] proposes a generative neural network for modeling ICU patient health based on HMMs. These studies differ from our approach of directly formulating HMMs as neural networks, which maintains the interpretability of HMMs while allowing for joint estimation of the HMM with other predictive models.

III. METHODS

In this section, we briefly review HMM preliminaries, formally define the HMRNN, and prove that it optimizes the same likelihood function as a corresponding HMM.

A. HMM preliminaries

Formally, an HMM models a system over a given time horizon T , where the system occupies a hidden state $x_t \in S = \{1, 2, \dots, k\}$ at any given time point $t \in \{0, 1, \dots, T\}$; that is, $x_t = i$ indicates that the system is in the i -th state at time t . For any state $x_t \in S$ and any time point $t \in \{0, 1, \dots, T\}$, the system emits an observation according to an emission distribution that is uniquely defined for each state. We consider the case of categorical emission distributions, which are commonly used in healthcare (e.g., [2], [12]). These systems emit a discrete-valued observation $y_t \in O$ at each time t , where $O = \{1, \dots, c\}$.

Thus, an HMM is uniquely defined by a k -length initial probability vector π , $k \times k$ transition matrix \mathbf{P} , and $k \times c$ emission matrix Ψ . Entry i in the vector π is the probability of starting in state i , row i in the matrix \mathbf{P} is the state transition probability distribution from state i , and row i of the matrix Ψ is the emission distribution from state i . We also define $\text{diag}(\Psi_i)$ as a $k \times k$ diagonal matrix with the i -th column of Ψ as its entries (i.e., the probabilities of observation i from each state). We define the likelihood of an observation sequence \mathbf{y} in terms of $\alpha_t(i)$, the probability of being in state i at time t and having observed $\{y_0, \dots, y_t\}$. We denote α_t as the (row) vector of all $\alpha_t(i)$ for $i \in S$, with

$$\alpha_t = \pi^\top \cdot \text{diag}(\Psi_{y_0}) \cdot \left(\prod_{i=1}^t \mathbf{P} \cdot \text{diag}(\Psi_{y_i}) \right) \quad (1)$$

for $t \in \{1, \dots, T\}$, with $\alpha_0 = \pi^\top \cdot \text{diag}(\Psi_{y_0})$. The likelihood of a sequence \mathbf{y} is thus given by $\Pr(\mathbf{y}) = \alpha_T \cdot \mathbf{1}_{k \times 1}$.

B. HMRNN definition

An HMRNN is a recurrent neural network whose parameters directly correspond to the initial state, transition, and emission probabilities of an HMM. As such, training an HMRNN optimizes the joint log-likelihood of the N T -length observation sequences given these parameters.

Definition III.1. *An HMRNN is a recurrent neural network with parameters π (a k -length vector whose entries sum to 1), \mathbf{P} (a $k \times k$ matrix whose rows sum to one), and Ψ (a $k \times c$ matrix whose rows sum to one). It receives $T + 1$ input matrices of size $N \times c$, denoted by \mathbf{Y}_t for $t \in \{0, 1, \dots, T\}$, where the n -th row of matrix \mathbf{Y}_t is a one-hot encoded vector of observation $y_t^{(n)}$ for sequence $n \in \{1, \dots, N\}$. The HMRNN consists of an inner block of hidden layers that is looped $T + 1$ times (for $t \in \{0, 1, \dots, T\}$), with each loop containing hidden layers $\mathbf{h}_1^{(t)}$, $\mathbf{h}_2^{(t)}$, and $\mathbf{h}_3^{(t)}$, and a c -length input layer $\mathbf{h}_y^{(t)}$ through which the input matrix \mathbf{Y}_t enters the model. The HMRNN has a single output unit $o^{(T)}$ whose value is the joint negative log-likelihood of the N observation sequences under an HMM with parameters π , \mathbf{P} , and Ψ ; the summed value of $o^{(T)}$ across all N observation sequences is the loss function (minimized via neural network optimization, such as gradient descent).*

Layers $\mathbf{h}_1^{(t)}$, $\mathbf{h}_2^{(t)}$, $\mathbf{h}_3^{(t)}$, and $o^{(T)}$ are defined in the following equations. Note that the block matrix in equation (3) is a

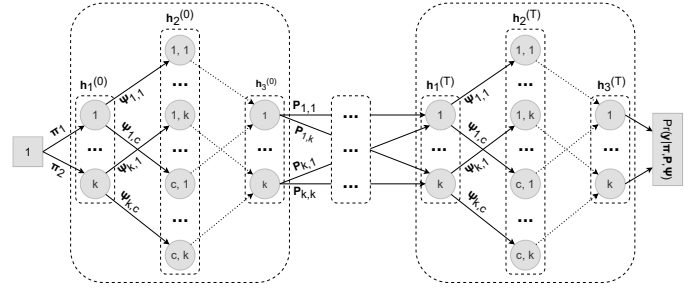


Fig. 1. Structure of the hidden Markov recurrent neural network (HMRNN). Solid lines indicate learned weights that correspond to HMM parameters; dotted lines indicate weights fixed to 1. The inner block initializes with the initial state probabilities then mimics multiplication by $\text{diag}(\Psi_{y_t})$; connections between blocks mimic multiplication by \mathbf{P} .

$c \times (kc)$ block matrix of c $\mathbf{1}_{1 \times k}$ vectors, arranged diagonally, while the block matrix in equation (4) is a $(kc) \times k$ row-wise concatenation of c $k \times k$ identity matrices.

$$\mathbf{h}_1^{(t)} = \begin{cases} \pi^\top, & t = 0, \\ \mathbf{h}_3^{(t-1)} \mathbf{P}, & t > 0. \end{cases} \quad (2)$$

$$\mathbf{h}_2^{(t)} = \text{ReLu} \left(\mathbf{h}_1^{(t)} \left[\text{diag}(\Psi_1) \dots \text{diag}(\Psi_c) \right] + \right. \quad (3)$$

$$\left. \mathbf{Y}_t \begin{bmatrix} \mathbf{1}_{1 \times k} & \dots & \mathbf{0}_{1 \times k} \\ \dots & \dots & \dots \\ \mathbf{0}_{1 \times k} & \dots & \mathbf{1}_{1 \times k} \end{bmatrix} - \mathbf{1}_{n \times (kc)} \right)$$

$$\mathbf{h}_3^{(t)} = \mathbf{h}_2^{(t)} \left[\mathbf{I}_k \dots \mathbf{I}_k \right]^\top \quad (4)$$

$$o^{(t)} = -\log(\mathbf{h}_3^{(T)} \mathbf{1}_{k \times 1}). \quad (5)$$

Fig. 1 outlines the structure of the HMRNN. Note that layer $\mathbf{h}_3^{(t)}$ is equivalent to α_t , the probability of being in each hidden state given $\{y_0, \dots, y_t\}$. Also note that, for long sequences, underflow can be addressed by normalizing layer $\mathbf{h}_3^{(t)}$ to sum to 1 at each time point, then simply subtracting the logarithm of the normalization term (i.e., the log-sum of the activations) from the output $o^{(T)}$.

C. Proof of HMM/HMRNN equivalence

We now formally establish that the HMRNN's output unit, $o^{(T)}$, is the negative log-likelihood of an observation sequence under an HMM with parameters π , \mathbf{P} , and Ψ . We prove this for the case of $N = 1$ and drop notational dependence on n (i.e., we write $y_t^{(1)}$ as y_t), though extension to $N > 1$ is trivial since the log-likelihood of multiple independent sequences is the sum of their individual log-likelihoods. We first rely on the following lemma.

Lemma III.1. *If all units in $\mathbf{h}_1^{(t)}(j)$ are between 0 and 1 (inclusive), then $\mathbf{h}_3^{(t)} = \mathbf{h}_1^{(t)} \text{diag}(\Psi_{y_t})$.*

Proof. Let $\mathbf{h}_1^{(t)}(j)$ and $\mathbf{h}_3^{(t)}(j)$ represent the j th units of layer $\mathbf{h}_1^{(t)}$ and $\mathbf{h}_3^{(t)}$, respectively, and recall that $\mathbf{h}_2^{(t)}$ contains $k \times c$ units, which we index with a tuple (l, m) for $l \in \{1, \dots, c\}$ and $m \in \{1, \dots, k\}$. According to equation (3), the connection between units $\mathbf{h}_1^{(t)}(j)$ and $\mathbf{h}_2^{(t)}(l, m)$ is $\Psi_{j,l}$ when $j = m$,

and 0 otherwise. Also recall that matrix \mathbf{Y}_t enters the model through a c -length input layer that we denote $\mathbf{h}_y^{(t)}$. According to equation (4), the connection between unit $\mathbf{h}_y^{(t)}(j)$ and unit $\mathbf{h}_2^{(t)}(l, m)$ is 1 when $j = l$, and 0 otherwise. Thus, unit $\mathbf{h}_2^{(t)}(l, m)$ depends only on $\Psi_{m,l}$, $\mathbf{h}_1^{(t)}(m)$, and $\mathbf{h}_y^{(t)}(l)$. Lastly, a bias of -1 is added to all units in $\mathbf{h}_2^{(t)}$, which is then subject to a ReLu activation, resulting in the following expression for each unit in $\mathbf{h}_2^{(t)}$:

$$\mathbf{h}_2^{(t)}(l, m) = \text{ReLu}(\Psi_{m,l} \cdot \mathbf{h}_1^{(t)}(m) + \mathbf{h}_y^{(t)}(l) - 1). \quad (6)$$

Because $\mathbf{h}_y^{(t)}(l)$ is 1 when $y_t = l$, and equals 0 otherwise, then if all units in $\mathbf{h}_1^{(t)}$ are between 0 and 1, this implies $\mathbf{h}_2^{(t)}(l, m) = \Psi_{m,l} \cdot \mathbf{h}_1^{(t)}(m)$ when $j = y_t$ and $\mathbf{h}_2^{(t)}(l, m) = 0$ otherwise. According to equation (5), the connection between $\mathbf{h}_2^{(t)}(l, m)$ and $\mathbf{h}_3^{(t)}(j)$ is 1 if $j = m$, and 0 otherwise. Hence,

$$\mathbf{h}_3^{(t)}(j) = \sum_{l=0}^c \mathbf{h}_2^{(t)}(l, j) = \Psi_{j,y_t} \cdot \mathbf{h}_1^{(t)}(j). \quad (7)$$

Thus, $\mathbf{h}_3^{(t)} = \mathbf{h}_1^{(t)} \text{diag}(\Psi_{y_t})$. \square

Theorem III.1. *An HMRNN with parameters π ($1 \times k$ stochastic vector), \mathbf{P} ($k \times k$ stochastic matrix), and Ψ ($k \times c$ stochastic matrix), and with layers defined as in equations (2-5), produces output neuron $o^{(T)}$ whose value is the negative log-likelihood of a corresponding HMM.*

Proof. Note that, based on Lemma III.1 and equation (2), $\mathbf{h}_3^{(t)} = \mathbf{h}_3^{(t-1)} \cdot \mathbf{P} \cdot \text{diag}(\Psi_{y_t})$ for $t \in \{1, \dots, T\}$, assuming that $\mathbf{h}_1^{(t)}(j) \in [0, 1]$ for $j \in \{1, \dots, k\}$. Since $\alpha_t = \alpha_{t-1} \cdot \mathbf{P} \cdot \text{diag}(\Psi_{y_t})$, then if $\mathbf{h}_3^{(t-1)} = \alpha_{t-1}$, then $\mathbf{h}_1^{(t)}(j) \in [0, 1]$ for $j \in \{1, \dots, k\}$ and therefore $\mathbf{h}_3^{(t)} = \alpha_t$. We show the initial condition that $\mathbf{h}_3^{(0)} = \alpha_0$, since $\mathbf{h}_1^{(0)} = \pi^\top$ implies that $\mathbf{h}_3^{(0)} = \pi^\top \cdot \text{diag}(\Psi_{y_0}) = \alpha_0$. Therefore, by induction, $\mathbf{h}_3^{(T)} = \alpha_T$, and $o^{(T)} = -\log(\alpha_T \cdot \mathbf{1}_{k \times 1})$, which is the logarithm of the HMM likelihood based on equation (1). \square

IV. EXPERIMENT AND RESULTS

We demonstrate how combining an HMRNN with other predictive neural networks improves predictive accuracy and offers novel clinical interpretations over a standard HMM, using an Alzheimer’s disease case study. We test our HMRNN on clinical data from $n = 426$ patients with mild cognitive impairment (MCI), collected over the course of three ($n = 91$), four ($n = 106$), or five ($n = 229$) consecutive annual clinical visits [13]. Given MCI patients’ heightened risk of Alzheimer’s, modeling their symptom progression is of considerable clinical interest. We analyze patients’ overall cognitive functioning based on the Mini Mental Status Exam (MMSE; [14]).

MMSE scores range from 0 to 30, with score categories for ‘no cognitive impairment’ (scores of 27-30), ‘borderline cognitive impairment’ (24-26), and ‘mild cognitive impairment’ (17-23) [15]. Scores below 17 were infrequent (1.2%) and were treated as scores of 17 for analysis. We use a 3-state latent space $S = \{0, 1, 2\}$, with $x_t = 0$ representing ‘no cognitive impairment,’ $x_t = 1$ representing ‘borderline

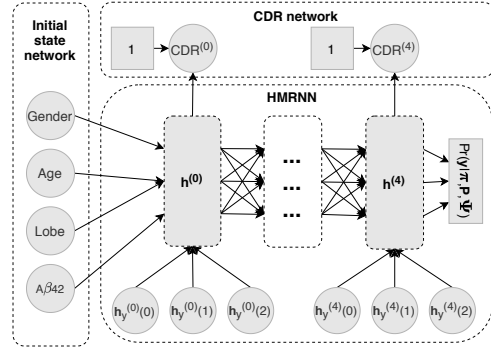


Fig. 2. Augmented HMRNN for Alzheimer’s case study. $\text{CDR}^{(t)}$ refers to predicted CDR classification (above or below 0.5) at time $t \in \{0, 1, 2, 3, 4\}$. ‘Lobe’ refers to measure of temporal lobe atrophy. Units $\mathbf{h}_y^{(t)}$ are a one-hot encoded representation of the MMSE score category at time t .

cognitive impairment,’ and $x_t = 2$ representing ‘mild cognitive impairment.’ The observation space is $O = \{0, 1, 2\}$, using $y_t = 0$ for scores of 27 – 30, $y_t = 1$ for scores of 24 – 26, and $y_t = 2$ for scores of 17 – 23. This HMM therefore allows for the possibility of measurement error, i.e., that patients’ observed score category y_t may not correspond to their true diagnostic classification x_t .

To showcase the benefits of the HMRNN’s modularity, we augment it with two predictive neural networks. First, we predict patient-specific initial state probabilities based on gender, age, degree of temporal lobe atrophy, and amyloid-beta 42 levels ($A\beta_{42}$, a relevant Alzheimer’s biomarker [16]), using a single-layer neural network with a softmax activation. Second, at each time point, the probability of being in the most impaired state, $\mathbf{h}_t^{(1)}(2)$, is used to predict concurrent scores on the Clinical Dementia Rating (CDR, [17]), a global assessment of dementia severity, allowing another relevant clinical metric to inform parameter estimation. We use a single connection and sigmoid activation to predict patients’ probability of receiving a CDR score above 0.5 (corresponding to ‘mild dementia’). The HMRNN is trained via gradient descent to minimize $o^{(T)}$ from equation (5), plus the predicted negative log-likelihoods of patients’ CDR scores. Figure 2 visualizes the structure of this augmented HMRNN.

We compare the HMRNN to a standard HMM without these neural network augmentations, trained using Baum-Welch, an expectation-maximization algorithm [1]. We assess parameter solutions’ ability to predict patients’ final MMSE score categories from their initial score categories, using 10-fold cross-validation. We evaluate performance using weighted log-loss L , i.e., the average log-probability placed on each final MMSE score category. This metric accounts for class imbalance and rewards models’ confidence in their predictions, an important component of medical decision support [18]. We also report \bar{p} , the average probability placed on patients’ final MMSE scores (computed directly from L). We train all models using a relative log-likelihood tolerance of 0.001%. Runtimes for Baum-Welch and the HMRNN are 2.89 seconds and 15.24 seconds, respectively.

TABLE I

RESULTS FROM ALZHEIMER'S DISEASE CASE STUDY. π IS INITIAL STATE DISTRIBUTION, P IS STATE TRANSITION MATRIX, Ψ IS EMISSION DISTRIBUTION MATRIX, L IS WEIGHTED LOG-LOSS, AND \bar{p} IS AVERAGE PROBABILITY PLACED ON GROUND TRUTH SCORE CATEGORIES.

| | Baum-Welch | | | HMRNN | | |
|-----------|------------|-------|-------|--------|-------|-------|
| π | 0.727 | 0.271 | 0.002 | 0.667 | 0.333 | 0.000 |
| P | 0.898 | 0.080 | 0.022 | 0.970 | 0.028 | 0.002 |
| | 0.059 | 0.630 | 0.311 | 0.006 | 0.667 | 0.327 |
| | 0.000 | 0.016 | 0.984 | 0.000 | 0.003 | 0.997 |
| Ψ | 0.939 | 0.060 | 0.001 | 0.930 | 0.067 | 0.003 |
| | 0.175 | 0.819 | 0.006 | 0.449 | 0.548 | 0.003 |
| | 0.004 | 0.160 | 0.836 | 0.005 | 0.308 | 0.687 |
| L | -0.992 | | | -0.884 | | |
| \bar{p} | 0.371 | | | 0.413 | | |

Model results appear in Table I. Note that the HMRNN's weighted log-loss L is significantly lower than Baum-Welch's (paired t -test p -value = 2.396×10^{-6}), implying greater predictive performance. Interestingly, the HMRNN yields lower transition probabilities and lower estimated diagnostic accuracy for the MMSE (i.e., lower diagonal values of Ψ) than Baum-Welch, suggesting that score changes are more likely attributable to testing error as opposed to true state changes.

V. DISCUSSION

The HMRNN can be combined with other neural networks to improve predictive accuracy in disease progression applications when additional patient data is available. In our case study, augmenting an HMRNN with two predictive networks improves forecasting performance compared with a standard HMM trained with Baum-Welch. Interestingly, the HMRNN yields a clinically distinct parameter interpretation, predicting poor diagnostic accuracy for the 'borderline' and 'mild' cognitive impairment states of the MMSE. This suggests that fewer diagnostic categories might improve the MMSE's utility, which is supported by existing research (e.g., [15]), and suggests the HMRNN might be used to improve the clinical utility of HMM parameter solutions. We also make a novel theoretical contribution by formulating discrete-observation HMMs as a special case of RNNs and by proving coincidence of their likelihood functions.

Future work might formally assess HMRNN time complexity. Yet since sequence lengths in healthcare are often considerably shorter than in other domains that employ HMMs (e.g., speech analysis), runtimes will likely be reasonable for many healthcare datasets. Future work might explore the HMRNN in other healthcare applications besides disease progression.

ACKNOWLEDGMENT

This research is partially supported by the Joint Directed Research and Development program at Science Alliance, University of Tennessee. Data collection and sharing for this project was funded by the Alzheimer's Disease Neuroimaging Initiative (ADNI) (National Institutes of Health Grant U01 AG024904) and DOD ADNI (Department of Defense award number W81XWH-12-2-0012).

This manuscript has been authored by UT-Battelle, LLC, under contract DE-AC05-00OR22725 with the US Department of Energy (DOE). The US government retains and the publisher, by accepting the article for publication, acknowledges that the US government retains a nonexclusive, paid-up, irrevocable, worldwide license to publish or reproduce the published form of this manuscript, or allow others to do so, for US government purposes. DOE will provide public access to these results of federally sponsored research in accordance with the DOE Public Access Plan (<http://energy.gov/downloads/doe-public-access-plan>). This research was sponsored by the Laboratory Directed Research and Development Program of Oak Ridge National Laboratory, managed by UT-Battelle, LLC, for the US Department of Energy under contract DE-AC05-00OR22725.

REFERENCES

- [1] L. Baum and T. Petrie, "Statistical inference for probabilistic functions of finite state Markov chains," *The Annals of Mathematical Statistics*, vol. 37, no. 6, pp. 1554–1563, 1966.
- [2] I. Stanculescu, C. Williams, and Y. Freer, "Autoregressive hidden Markov models for the early detection of neonatal sepsis," *IEEE Journal of Biomedical and Health Informatics*, vol. 18, no. 5, pp. 1560–1570, 2013.
- [3] Y. Liu, S. Li, F. Li, L. Song, and J. Rehg, "Efficient learning of continuous-time hidden Markov models for disease progression," *Advances in Neural Information Processing Systems*, pp. 3600–3608, 2015.
- [4] S. Nemat, M. Ghassemi, and G. Clifford, "Optimal medication dosing from suboptimal clinical examples: A deep reinforcement learning approach," *38th Annual International Conference of IEEE Engineering in Medicine and Biology Society*, pp. 2978–2981, 2016.
- [5] Z. Zhou, Y. Wang, H. Mamani, and D. Coffey, "How do tumor cytogenetics inform cancer treatments? dynamic risk stratification and precision medicine using multi-armed bandits," *Preprint*, 2019.
- [6] T. Rydén, "Em versus markov chain monte carlo for estimation of hidden markov models: A computational perspective," *Bayesian Analysis*, vol. 3, no. 4, pp. 659–688, 2008.
- [7] T. Caelli, L. Guan, and W. Wen, "Modularity in neural computing," *Proceedings of the IEEE*, vol. 87, no. 9, pp. 1497–1518, 1999.
- [8] T. Wessels and C. Omlin, "Refining hidden Markov models with recurrent neural networks," in *Proceedings of the IEEE-INNS-ENNS International Joint Conference on Neural Networks*, vol. 2, 2000, pp. 271–276.
- [9] J. Bridle, "Alpha-nets: A recurrent 'neural' network architecture with a hidden Markov model interpretation," *Speech Communication*, vol. 9, no. 1, pp. 83–92, 1990.
- [10] B. Estebanez, P. del Saz-Orozco, I. Rivas, E. Bauzano, V. Muñoz, and I. Garcia-Morales, *Maneuvers recognition in laparoscopic surgery: Artificial Neural Network and hidden Markov model approaches*. IEEE, 2012, pp. 1164–1169.
- [11] M. Baucum, A. Khojandi, and R. Vasudevan, "Improving deep reinforcement learning with transitional variational autoencoders: A healthcare application," *Journal of Biomedical & Health Informatics (forthcoming)*, 2020.
- [12] T. Ayer, O. Alagoz, and N. Stout, "A POMDP approach to personalize mammography screening decisions," *Operations Research*, vol. 60, no. 5, pp. 1019–1034, 2012.
- [13] A. D. N. Initiative, "Alzheimer's disease neuroimaging initiative," adni.loni.usc.edu.
- [14] M. Folstein, S. Folstein, and P. McHugh, "Mini-mental state: A practical method for grading the cognitive state of patients for the clinician," *Journal of Psychiatric Research*, vol. 12, no. 3, pp. 189–198, 1975.
- [15] T. Monroe and M. Carter, "Using the Folstein mini mental state exam (MMSE) to explore methodological issues in cognitive aging research," *European Journal of Ageing*, vol. 9, no. 3, pp. 265–274, 2012.
- [16] K. Blennow, "Cerebrospinal fluid protein biomarkers for Alzheimer's disease," *NeuroRx*, vol. 1, no. 2, pp. 213–225, 2004.
- [17] J. Morris, "Clinical dementia rating: Current version and scoring rules," *Neurology*, vol. 43, pp. 2412–2414, 1993.
- [18] A. Bussone, S. Stumpf, and D. O'Sullivan, *The role of explanations on trust and reliance in clinical decision support systems*, 2015, pp. 160–169.